*Earthquake Engineering, Tenth World Conference © 1992 Balkema, Rotterdam. ISBN 90 5410 060 5*

# Earthquake energy partitioning in bridge structures with seismic isolators

H. Iemura
*Department of Civil Engineering, Kyoto University, Japan*

K. Ohshima
*Hanshin Expressway Public Corporation, Kobe, Japan*

T. Nakata
*Yachiyo Engineering Consultants, Osaka, Japan*

ABSTRACT: New earthquake energy spectra are proposed for practical design procedures using energy concepts. The spectra show integrated earthquake input energy of a unit mass for a given natural period and damping ratio. The total input energy and its partitioning in complex structures can be evaluated with conventional procedure of modal analysis and the proposed spectra. Numerical simulations are carried out for inelastic structures to show the earthquake energy partitioning in time and in space. Inelastic earthquake response and earthquake energy partitioning of bridge structures with and without seismic isolators subjected to earthquake ground motions is evaluated to verify their engineering significance.

## 1 EARTHQUAKE INPUT ENERGY SPECTRA

Equation of motion of a single-degree-of-freedom inelastic structure with mass $m$, damping coefficient $C$, and hysteretic restoring force $F(x)$, subjected to earthquake ground acceleration $\ddot{z}$ is

$$m\ddot{x} + C\dot{x} + F(x) = -m\ddot{z} \tag{1}$$

Multiplying by $dx(= \dot{x}dt)$ and integrating each term of Eq. (1) for the duration of earthquake ground motion $(0 \sim t_0)$, it follows that

$$\frac{1}{2}m\dot{x}^2(t_0) + \int_0^{t_0} C\dot{x}^2 dt \quad + \quad \int_0^{t_0} F(x)\dot{x}dt = -\int_0^{t_0} m\dot{x}(t)\ddot{z}dt \tag{2}$$

The first term on the left-hand side of Eq. (2) represents the kinetic energy of the mass at time $t_0$, the second term is the energy absorbed by viscous damping during vibration, and the third term includes both accumulated and dissipated energy by the hysteresis loops of the restoring force up to time $t_0$. On the right-hand side of Eq. (2) is the earthquake input energy to a structure from time 0 to $t_0$.

Partitioning of the earthquake energy in time domain, represented by Eq. (2), is shown in Figs. 1 and 2 for a single DOF linear structure (T=0.5s, $\xi$=0.01), respectively. NS component of the El Centro record during the 1940 Imperial Valley Earthquake is used as input and hysteresis loops of a high-damping rubber bearing are used in the computer-actuator on-line hybrid earthquake response simulation (Iemura et al). Comparing the results, it is clearly found that the earthquake input energy $E$, the kinetic energy $W_k$ and the potential energy $W_E$ are suppressed to much lower level by the effect of base isolation bearing.

The earthquake input energy to a linear SDOF system with a unit mass at the end of excitation is a function of natural period and of damping factor. Analogous to conventional response spectra, it is named as "the earthquake input response spectra".

## 2 ENERGY PARTITIONING IN COMPLEX STRUCTURES

For a MDOF structure, its energy partitioning can be written as

$$\sum_i \left(\frac{1}{2}m_i\dot{x}_i^2\right) + \sum_i \int_0^{t_0} C_i\dot{y}_i^2 dt \quad + \quad \sum_i \int_0^{t_0} F_i\dot{y}_i dt = \sum_i \int_0^{t_0} (-m\dot{x}_i\ddot{z})dt \tag{3}$$

where $i$ denotes the $i$-th mass or the $i$-th interstory, $x$ and $y$ denote relative displacement to ground and interstory displacement, respectively. Eq. (3) can also be written as

$$\sum_i W_{K_i} + \sum_i W_{C_i} + \sum_i W_{E_i} + \sum_i W_{H_i} = \sum_i E_i \tag{4}$$

At the end of response, kinetic and potential energies vanish, and thus the total input energy is absorbed by both viscous and hysteretic damping.

Using the modal analysis procedure and the proposed earthquake input energy spectra, the total earthquake input energy to an equivalent linear MDOF structure can be described by

$$\sum_i \int_0^{t_0} (-m\dot{x}_i \ddot{z}) dt = \sum_i \left\{ -m_i \int_0^{t_0} \left( \sum_s \phi_{is} \dot{y}_s \right) \ddot{z} \right\} dt = \sum_i m_i \left( \sum_s \phi_{is} E_s \right) \quad (5)$$

where $E_s$ is the earthquake input energy in $s$-th mode. $E_s$ can be found from the proposed energy spectra. When there is no modal coupling, the earthquake input energy estimated by Eq. (5) agrees perfectly with the results of step-by-step numerical calculation. Hence, analytical estimation of earthquake input energy and its partitioning can be carried out with application of equivalent linearization techniques.

## 3 INELASTIC EARTHQUAKE RESPONSE OF DIFFERENT BRIDGE MODELS

For numerical simulation of earthquake energy partitioning in bridge structures with and without seismic isolators, one of typical bridges used in Hanshin Expressway Public Corporation shown in Fig. 3(a) is adopted. A bridge consists of steel girder, reinforced concrete (RC) pier and pile foundation. They are modeled with flexure beam elements as shown in Fig. 3(b). Trilinear hysteretic restoring force characteristic is assumed for moment curvature $(M-\phi)$ relation of a pier. Pile foundation is modeled by horizontal and rotational elastic springs in accordance with the the earthquake design specification of highway bridges in Japan. Energy dissipation due to soil-structure interaction is modeled by 10% viscous damping.

The following four types of connection between the girder and the pier top are modeled and inserted between No. 12 and 10 mass in the model shown in Fig. 3(b).

1. Rotation-free pin connection (Model 1)
2. Elastic spring support of which natural frequency is set at 2.0 sec (Model 2)
3. Isolator with bilinear restoring force (model 3)
4. Elastic spring support with viscous damper (model 4)

As earthquake ground input motion, NS-component of the El Centro record during the 1940 Imperial Earthquake is adopted and maximum acceleration is scaled to 600 gal to represent an extremely large event.

Displacement response of a girder which is pin connected to a pier (Model 1) and moment-curvature $(M-\phi)$ hysteretic response of section No. 4 of pier bottom are shown in Fig. 4(a) and (b), respectively. Maximum displacement response of a girder is found to be 15.3 cm with vibration period of one second. Bending moment response of a section at the pier bottom goes deeply into plastic region, and deterioration of both resistance and stiffness is observed. Displacement and $(M-\phi)$ response of a bridge with elastic spring support (Model 2) are shown in Fig. 5(a) and (b). Although large displacement (35cm) is found due to soft elastic spring support, moment response at the pier bottom shows much less hysteretic behavior. Fig. 6(a) and (b) show displacement and $(M-\phi)$ response of a bridge with an isolator with bilinear hysteretic restoring characteristics (Model 3). Fig. 7(a) and (10) show response of a bridge with elastic spring support and viscous damper (Model 4). In both models 3 and 4, much smaller hysteretic behavior is found compared to pin connection. Maximum displacement (20cm for Model 3, 10cm for Model 4) is also found smaller than Model 2.

Spatial distribution of maximum displacement response and acceleration and maximum bending moment response is plotted Fig. 8(a), (b), and (c). All displacement, acceleration response of a girder and bending moment response of a pier wih pin connection (Model 1) show much larger response than others (Models 2, 3 and 4). This verifies that pin connection gives higher seismic load to piers than other models. It shall be noticed that higher variation is found in displacement response of girders for seismic safety evaluation of bridges with various types of supports.

## 4 EARTHQUAKE ENERGY PARTITIONING IN BRIDGE STRUCTURES

Partitioning of earthquake input energy and absorbed energy in bridge structures are summarized in Table 1. Superstructures share large part of earthquake input energy due to their large masses. When elastic support (Model 2), bilinear isolator (Model 3) and viscous damper (Model 4) are used, earthquake input energy to girders is reduced significantly. Consequently, total input energy to bridge structures is also reduced significantly. The reason of this reduction is due to longer vibrational period of softly-snpported superstructures.

Earthquake input energy is absorbed by different strnctural members depending on different structural models. In pin connection (Model 1), earthquake response of a pier goes into inelastic region deeply and absorbs one-fifth of the total inpnt energy, which means that the pier has to accept some earthquake damage. In Model 2 of elastic support, all elements stays in elastic range and almost all of input energy is absorbed by soil-structure interaction. In Model 3 and 4, from one third to half of input energy is absorbed by the isolator or the damper. Consequently, hysteretic energy absorption by piers is reduced significantly which would then guarantee high reliability of bridge structures.

In all models, large part of the input energy is absorbed by soil-structure interaction. The simulated results of this study, including different level and types of earthquake response, will be used for practical design of energy-absorbing capacity of seismic isolators.

## 5 CONCLUSIONS

To develop earthquake energy based design concept, the new earthquake energy spectra are proposed. Analytical control of partitioning of the earthquake energy in base-isolated structures has become possible with the use of the spectral and modal analysis of equivalently linearized systems. Effects of inelastic behavior of isolators and of dynamic dampers are evaluated from numerical smiulations. Appropriately designed isolators are found not only to suppress earthquake input energy but also to absorb most of it, thus, reducing the structural damage significantly.

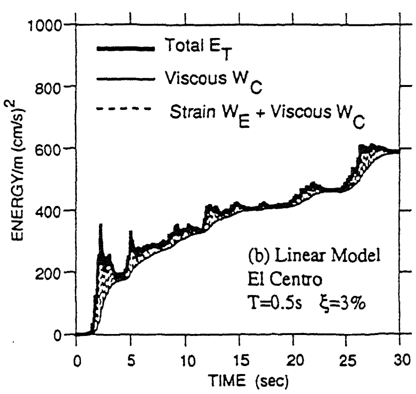


Fig. 1 Energy Partitioning in a Linear SDOF Structure

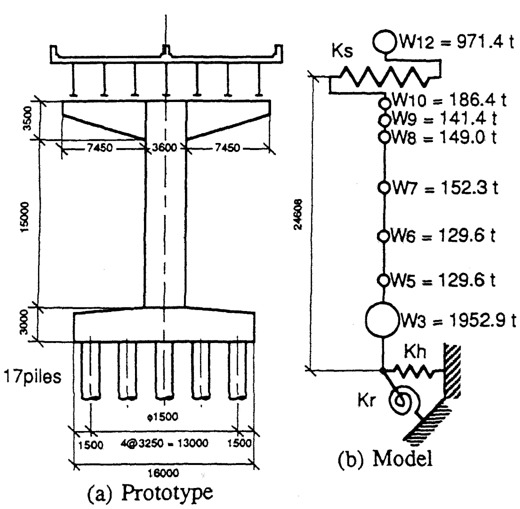


Fig. 3 Prototype and Model of a Bridge Structure

## REFERENCES


B. Kato and H. Akiyama, "Energy Input and Damages in Structures Subjected to Severe Earthquakes," Proc., AIJ, No. 235, 9-18,1985. (in Japanese)

T. Ohno, et al, "Quantative Estimation of Plastic Energy Absorbed in Structures Subjected to Seismic Excitation," Proc., JSCE No. 333, 91-99, May, 1983. (in Japanese)

H. Iemura, "Hybrid Experiments on Earthquake Failure Criteria of Reinforced Concrete Structures," Proc., 6th WCEE, VI, 103-110, (1984).

H. Iemura, et al, "Reduced DOF Approxmiations for Earthquake Damage Assessments of Deteriorating Hysteretic Structures," Proc., 6th JEES, 1233-1240, Dec. 1982.

H. Iemura, et al, "On-line Earthquake Response Tests of High-Damping Rubber Bearings for Seismic Isolation," Proc. of the 1st US-Japan Workshop on Earthquake Protective Systems for Bridges, Sept., 1991. (in printing)


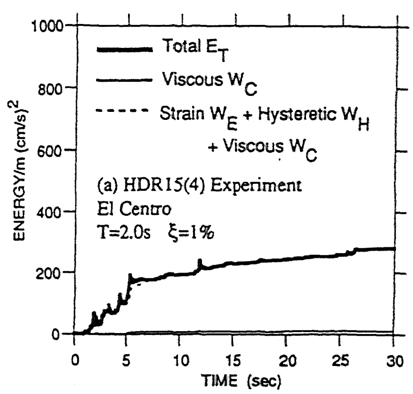


Fig. 2 Energy Partitioning in a Base-Isolated Structure

Table–1 Spatial Partitioning of Earthquake Input Energy and Absorbed Energy in Bridge Structures

| Energy Partioning \ Types of Supports | | Pin Connection | Elastic Supports | Bilinear Isolator | Viscous Damper |
|---|---|---|---|---|---|
| Earthquake Imput Energy | Super Structures | 22 550 | 10 400 | 9 912 | 16 460 |
| | Piers | 14 070 | 8 473 | 10 130 | 10 550 |
| | Foundations | 9 613 | 6 556 | 7 947 | 6 752 |
| | Total | 46 230 | 25 430 | 27 990 | 33 760 |
| Hysteretic Energy Absorption | Bearings | 0 | 0 | 8 661 | 16 710 |
| | Piers | 10 210 | 229 | 46 | 293 |
| | Foundations | 0 | 0 | 0 | 0 |
| | Sub Total | 10 210 | 230 | 8 710 | 17 000 |
| Viscous Energy Absorption | | 36 860 | 25 200 | 19 180 | 16 750 |
| Total of Absorbed Energy | | 47 070 | 25 430 | 27 890 | 33 750 |

Unit : (t · cm)

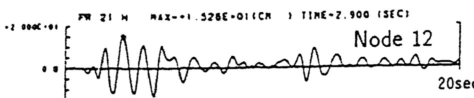


(a) Displacement Response of Girder

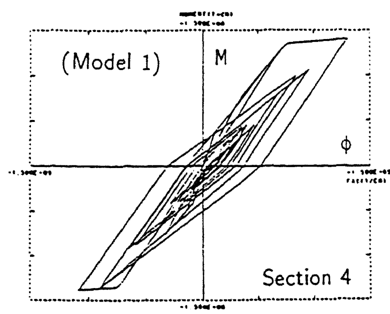


(b) $M - \phi$ Response of Pier Model

Fig. 4 Bridge Model with Pin Connection

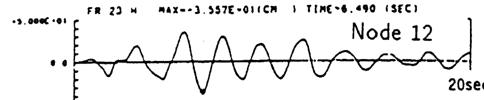


(a) Displacement Response of Girder

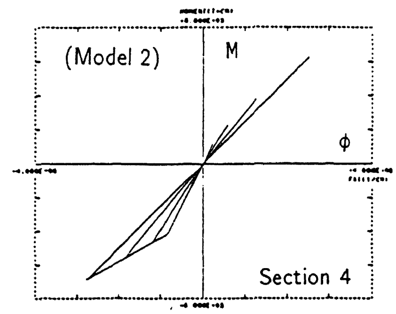


(b) $M - \phi$ Response of Pier Model

Fig. 5 Bridge Model with Elastic Spring Support

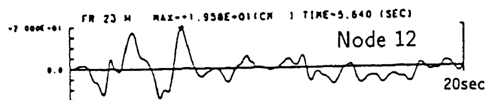


(a) Displacement Response of Girder

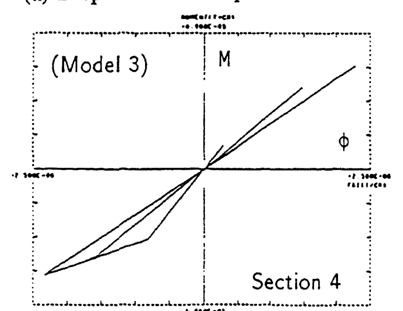


(b) $M - \phi$ Response of Pier Model

Fig. 6 Bridge Model with Bilinear Hysteresis Isolator

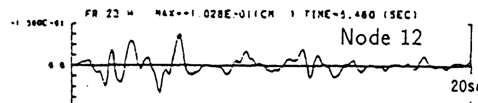


(a) Displacement Response of Girder

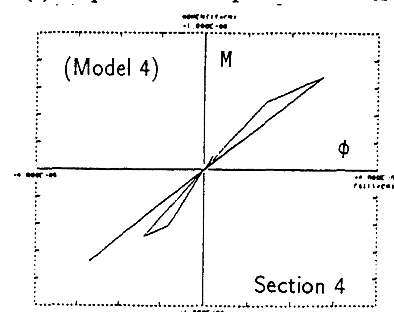


(b) $M - \phi$ Response of Pier Model

Fig. 7 Bridge Model with Viscous Damper

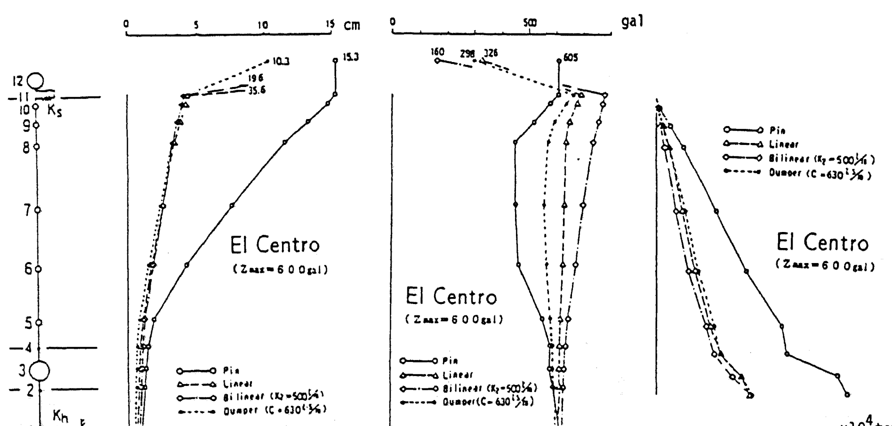


(a) Maximum Displacement (b) Maximum Acceleration

Fig. 8 Spatial Distribution of Maximum Response (c) Maximum Bending Moment